https://doi.org/10.5194/amt-2020-316
Preprint. Discussion started: 4 September 2020

Atmospheric Measurement Techniques Discussions

Characterisation and potential for reducing optical resonances in FTIR spectrometers of the Network for the Detection of Atmospheric Composition Change (NDACC)

Thomas Blumenstock[1], Frank Hase[1], Axel Keens[2], Denis Czurlok[2], Orfeo Colebatch[3], Omaira Garcia[4], David W. T. Griffith[5], Michel Grutter[6], James W. Hannigan[7], Pauli Heikkinen[8], Pascal Jeseck[9], Nicholas Jones[5], Rigel Kivi[8], Erik Lutsch[3], Maria Makarova[10], Hamud Kh. Imhasin[10], Johan Mellqvist[11], Isamu Morino[12], Tomoo Nagahama[13], Justus Notholt[14], Ivan Ortega[7], Mathias Palm[14], Uwe Raffalski[15], Markus Rettinger[16], John Robinson[17], Matthias Schneider[1], Christian Servais[18], Dan Smale[17], Wolfgang Stremme[6], Kimberly Strong[3], Ralf Sussmann[16], Yao Té[9], Voltaire A. Velazco[5]

[1]Karlsruhe Institute of Technology (KIT), Institute of Meteorology and Climate Research (IMK-ASF), Karlsruhe, Germany
[2]Bruker Optics GmbH, Ettlingen, Germany
[3]Department of Physics, University of Toronto, Toronto, Canada
[4]Izaña Atmospheric Research Centre (IARC), Meteorological State Agency of Spain (AEMET), Tenerife, Spain
[5]Centre for Atmospheric Chemistry, University of Wollongong, Wollongong, Australia
[6]Centro de Ciencias de la Atmósfera, Universidad Nacional Autónoma de México (UNAM), Mexico City, México
[7]National Center for Atmospheric Research (NCAR), Boulder, CO, USA
[8]Finnish Meteorological Institute (FMI), Sodankylä, Finland
[9]Laboratoire d'Etudes du Rayonnement et de la Matière en Astrophysique et Atmosphères (LERMA-IPSL), Sorbonne Université, CNRS, Observatoire de Paris, PSL Université, 75005 Paris, France
[10]Saint Petersburg State University, Atmospheric Physics Department, St. Petersburg, Russia
[11]Department of Earth and Space Science, Chalmers University of Technology, Göteborg, Sweden
[12]National Institute for Environmental Studies (NIES), Tsukuba, Ibaraki 305-8506, Japan
[13]Institute for Space-Earth Environmental Research (ISEE), Nagoya University, Nagoya, Japan
[14]Institute of Environmental Physics, University of Bremen, Bremen, Germany
[15]Swedish Institute of Space Physics (IRF), Kiruna, Sweden
[16]Karlsruhe Institute of Technology, IMK-IFU, Garmisch-Partenkirchen, Germany
[17]National Institute of Water and Atmospheric Research Ltd (NIWA), Lauder, New Zealand
[18]Institut d'Astrophysique et de Géophysique, Université de Liège, Liège, Belgium

Correspondence to: Thomas Blumenstock (thomas.blumenstock@kit.edu)

Abstract. Although optical components in Fourier transform infrared (FTIR) spectrometers are preferably wedged, in practice, infrared spectra typically suffer from the effects of optical resonances ("channeling") affecting the retrieval of weakly absorbing gases. This study investigates the level of channeling of each FTIR spectrometer within the Network for the Detection of Atmospheric Composition Change (NDACC). Dedicated spectra were recorded by more than twenty NDACC FTIR spectrometers using a laboratory mid-infrared source and two detectors. In the InSb detector domain (1900 – 5000 cm^{-1}), we find that the amplitude of the most pronounced channeling frequency amounts to 0.1 to 2.0 ‰ of the spectral background level, with a mean of (0.68 ± 0.48) ‰ and a median of 0.60 ‰. In the HgCdTe detector domain (700 – 1300 cm^{-1}), we find

https://doi.org/10.5194/amt-2020-316
Preprint. Discussion started: 4 September 2020

Atmospheric Measurement Techniques Discussions

even stronger effects, with the largest amplitude ranging from 0.3 to 21 ‰ with a mean of (2.45 ± 4.50) ‰ and a median of 1.2 ‰. For both detectors, the leading channeling frequencies are 0.9 and 0.11 or 0.23 cm^{-1} in most spectrometers. These observed spectral frequencies correspond to the optical thickness of the air gap in between the beam splitter and compensator plate (0.9 cm^{-1}) and the beam splitter substrate itself (0.11 and 0.23 cm^{-1}). Since the air gap is a significant source of channeling and the corresponding amplitude differs strongly between spectrometers, we propose new beam splitters with the wedge of the air gap increased to at least 0.8°. We tested the insertion of spacers in a beam splitter's air gap to demonstrate that increasing the wedge of the air gap decreases the 0.9 cm^{-1} channeling amplitude significantly. This study shows the potential for reducing channeling in the FTIR spectrometers operated by the NDACC, thereby increasing the quality of recorded spectra across the network.

1 Introduction

Ground-based FTIR (Fourier transform infrared) spectroscopy is a widely used technique for measuring column abundances of a variety of trace gases in the atmosphere. Within the Network for the Detection of Atmospheric Composition Change (NDACC), this technique is used at about twenty sites covering a wide range of geographical latitudes. The NDACC data are used to study short and long-term variability of the atmosphere as well as for satellite data validation (De Mazière et al., 2018). For both applications, high data quality and station-to-station consistency are of utmost importance. Ground-based FTIR spectroscopy provides data of high quality (e.g. Schneider and Hase, 2008). However, several key instrumental characteristics need to be addressed. These parameters such as detector non-linearity (Abrams et al., 1994), instrumental line shape (ILS; Hase et al., 1999), intensity fluctuations (Keppel-Aleks et al., 2007), precise solar tracking (Gisi et al., 2011), and sampling error (Messerschmidt et al., 2010; Dohe et al., 2013) have been studied in some detail and need to be taken into account.

In this paper, channeling – the presence of instrument-induced periodic oscillations of spectral transmission resulting from internal optical resonances – will be investigated and discussed. In the past, each site or each new spectrometer was tested for channeling individually. This paper describes a network-wide exercise for characterizing channeling in FTIR spectrometers. Channeling is caused by interference of reflections of the incoming light at parallel transmitting surfaces of optical elements. In practice, the resulting channeling amplitudes are less than 1% in signal. Thus, the retrieved data for species with strong absorption signatures, as for example ozone and many others, are less critically affected. However, the retrieved trace gas amounts of weak absorbers can be substantially disturbed. In such cases, channeling becomes an important component of the total error budget.

Recently, time series of column abundances of formaldehyde (HCHO) were retrieved from NDACC FTIR sites (Vigouroux et al., 2018, 2020). The studies of Vigouroux also includes an error characterisation of the HCHO product. Within the network, two retrieval codes are in use: SFIT4 and PROFFIT. While the retrieval codes were inter-compared and show consistent results (Hase et al., 2004), the assumed error budgets differ slightly. The stations using PROFFIT include an error contribution due to channeling while the stations using SFIT4 do not. The result is a larger total error for HCHO data retrieved with PROFFIT as

https://doi.org/10.5194/amt-2020-316
Preprint. Discussion started: 4 September 2020

Atmospheric Measurement Techniques Discussions

compared to SFIT4 (Vigouroux et al., 2018). In the PROFFIT error calculation, a set of typical channeling frequencies and amplitudes is taken into account. More specifically, channeling amplitudes of 0.5 ‰ for four frequencies are assumed: 0.005, 0.2, 1.0, and 3.0 cm^{-1}. The resulting error contribution doubles the total error of HCHO columns amounts.

In order to make this assumption more robust and to quantify more carefully the differences from spectrometer to spectrometer, an exercise was performed to measure channeling frequencies and amplitudes of NDACC FTIR spectrometers. Since atmospheric spectra are densely populated with absorption signatures interfering with the signal generated by channeling; the test was designed using spectra collected in a laboratory setting. Section 2 briefly describes the origin of channeling, Sect. 3 the setup of this exercise, and Sect. 4 shows the results followed by a discussion. Finally, to reduce the channeling amplitude, the investigation of a modified beam splitter design is presented in Sect. 5, and lastly, Sect. 6 gives the conclusions.

2 Spectral transmission of a Fabry-Perot cavity

In an FTIR spectrometer, the transmitted light passes through several optical components such as optical windows, optical filters and a beam splitter, typically comprised of a beam-splitting layer system deposited on a transparent substrate and a compensator. At the transmitting surfaces of these components, the optical beam is partially reflected. In the case of parallel surfaces, each pair of surfaces defines a cavity (Fig. 1a) in which multiple reflections occur. Due to interference of the reflected light, a standing wave is created (Fig. 1b). This effect is called the Fabry-Perot or etalon effect or channeling. The optical length of the cavity defines the free spectral range $\nu_{(FSR)}$ as

$$\nu(FSR) = 1/(2ndcos\theta) \quad (1)$$

with n refractive index and d thickness of the optical component (Hecht, 2017). θ is the angle between incoming light beam and the normal of the optical surface (Fig. 1a). Equation (1) is used to assign the optical element responsible for a certain channeling frequency. Table 1 gives a few examples of $\nu_{(FSR)}$ for optical materials commonly used in FTIR spectrometers. The Fabry-Perot etalons generated by these undesired parasitic effects naturally have rather low etendue, so the resulting spectral transmission is well described by assuming an harmonic oscillation.

In order to reduce or avoid channeling, optical components need to be wedged or installed with a large tilt. A large tilt is not feasible in many cases. Thus, components are normally wedged, which requires a special design and limits compatibility with non-wedged devices. Furthermore, some components such as detector elements are not available as wedged versions (the partially transparent detector element can also act as optical cavity). Therefore, in practice it is challenging to design an FTIR spectrometer that is completely free of channeling.

https://doi.org/10.5194/amt-2020-316
Preprint. Discussion started: 4 September 2020

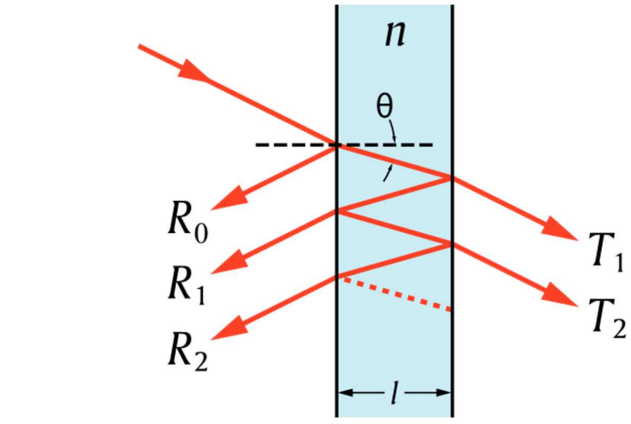

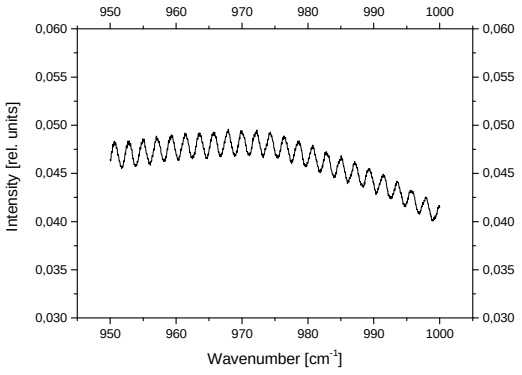

Figure 1: (a) Multiple reflections at parallel surfaces in an optical component (taken from Wikimedia Commons: https://commons.wikimedia.org/), (b) Channeling in an IR spectrum.

Table 1: Free spectral range $\nu_{(FSR)}$ of some components typically used in NDACC FTIR spectrometers.

Material	used as	*n*	*d* [mm]	$\nu_{(FSR)}$ [cm^{-1}]
Air	Gap in between beam splitter and compensator plate	1	5.5	0.91
KBr	Beam splitter substrate	1.5	15	0.22
CaF_2	Beam splitter substrate	1.4	15	0.24
CaF_2	Detector window	1.4	1.0	3.57
Ge	Detector window	4.4	1.0	1.14
KRS-5 (TlBr-TlI)	Detector window	2.37	1.0	2.11
Sapphire	Detector window	1.65	1.0	3.0
ZnSe	Detector window	2.2	1.0	2.27

https://doi.org/10.5194/amt-2020-316
Preprint. Discussion started: 4 September 2020


Atmospheric Measurement Techniques Discussions

110

3 Channeling test exercise

3.1 Experimental setup

In atmospheric spectra, channeling can be difficult to see due to the presence of complex atmospheric signatures. Therefore, laboratory spectra are used for this exercise, recorded either with a mid-infrared globar or with a black body of at least 1000 °C
115 temperature. Since these types of sources do not include a window, no additional channeling is added to the spectra. A temperature of 1000 °C is required to record spectra with a sufficient signal-to-noise ratio in a reasonable amount of time.

Within NDACC, two detectors and the NDACC filter set are used. The NDACC filters have a wedge of 10 arc min and therefore, if properly oriented, do not cause channeling. Therefore, not all filters but both detectors were included in this exercise. More specifically, NDACC filter #3 (2400 to 3000 cm^{-1} spectral range) for the InSb detector and NDACC filter #6
120 (700 to 1300 cm^{-1} spectral range) for the HgCdTe detector were used. Some sites use filter #7 (700 to 1000 cm^{-1} spectral range) and #8 (1000 to 1400 cm^{-1} spectral range) instead of filter #6. In this case, filter #7 was used for this exercise. Filter #3 was selected since this filter range is used for the retrieval of HCHO column abundances.

Multiple reflections within optical components such as optical windows or beam splitters typically show channeling frequencies of a few tenths of a wavenumber up to a few wavenumbers. In general, higher frequency channeling with
125 wavenumbers below 0.1 cm^{-1} might occur when different optical components form the surfaces of the resulting cavity, e.g. in the Bruker 120HR spectrometer the rim of the entrance field stop is part of a resonator of about 1 m length. However, this is seldom the case in an FTIR spectrometer and secondly, due to the high frequency, easily detectable even in atmospheric spectra.

In order to focus on channeling due to multiple reflections inside optical components and to achieve a very good signal-to-
130 noise ratio, a spectral resolution of 0.05 cm^{-1} was chosen. This resolution allowed us to add thousand interferograms within a few hours, thereby achieving signal-to-noise ratio that allowed channeling amplitudes to be detected and quantified on a per mille scale.

3.2 Analysis of channeling test spectra

To quantify channeling frequencies and their amplitudes, an FFT (Fast Fourier Transform) analysis of the spectra was
135 conducted. First of all, a spectral interval was chosen with a nearly constant intensity: 950 to 1000 cm^{-1} for HgCdTe and 2550 to 2600 cm^{-1} for InSb spectra. This step was carried out using OPUS™, a software package from Bruker Optics to control FTIR spectrometers (Fig. 2a). Then, the background was normalized and a straight line was subtracted using Origin™ software (Fig. 2b). Finally, an inverse FFT was conducted also with Origin™ software (Fig. 2c).

140

https://doi.org/10.5194/amt-2020-316
Preprint. Discussion started: 4 September 2020

Atmospheric Measurement Techniques Discussions

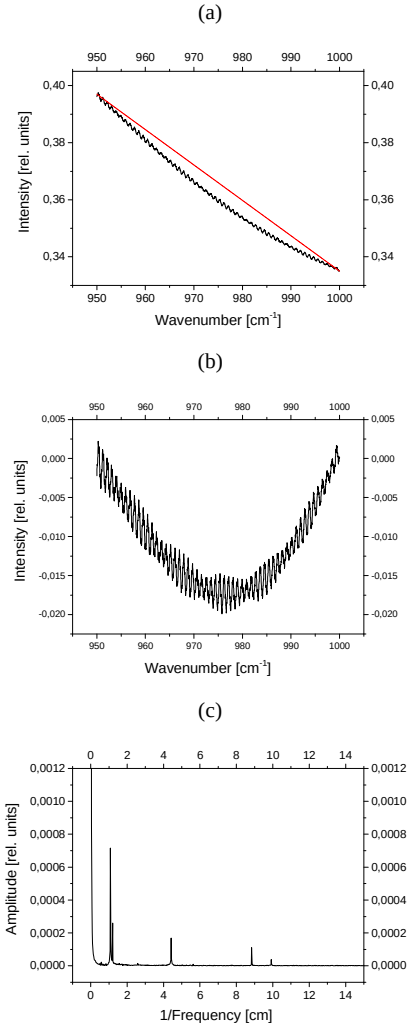

Figure 2: Analysis of a channeling test spectrum: (a) Cut off a window of 50 cm^{-1}; (b) Normalize background and subtract straight line; (c) Result of FFT analysis

4 Results and Discussion

In this section, the results are presented for more than twenty spectrometers. Table 2 provides the list of spectrometers included in this study. Please note that a few spectrometers do not include an HgCdTe detector: Garmisch, Karlsruhe, and Sodankylä.

https://doi.org/10.5194/amt-2020-316
Preprint. Discussion started: 4 September 2020

Atmospheric Measurement Techniques Discussions

Table 2: List of spectrometers contributing to the channeling test exercise, sorted by latitude of the site, from north (Eureka) to south (Arrival Heights).

Site	Acronym	Type	Beam splitter setup	Team
Eureka	EUR	Bruker 125 HR	KBr	U Toronto
Ny-Ålesund	NY	Bruker 120/5 HR	KBr for HgCdTe, CaF_2 for InSb det.	U Bremen
Thule	THU	Bruker 125 HR	KBr	NCAR
Kiruna	KIR	Bruker 120/5 HR	KBr	KIT-ASF, IRF
Sodankylä	SOD	Bruker 125 HR	CaF_2, no HgCdTe det.	FMI
Harestua	HAR	Bruker 120 M	KBr	U Gothenborg
St. Petersburg	STP	Bruker 120 HR	KBr	SPbU
Bremen	BRE	Bruker 125 HR	KBr	U Bremen
Karlsruhe	KAR	Bruker 125 HR	CaF_2, no HgCdTe det.	KIT-ASF
Paris	PAR	Bruker 125 HR	KBr for HgCdTe, CaF_2 for InSb det.	Sorbonne U
Garmisch	GAR	Bruker 125 HR	CaF_2, no HgCdTe det.	KIT-IFU
Zugspitze	ZUG	Bruker 120/5 HR	KBr	KIT-IFU
Jungfraujoch	JJO	Bruker 120 HR	KBr	U Liège
Toronto	TOR	BOMEM DA8	KBr	U Toronto
Rikubetsu	RIK	Bruker 120/5 HR	KBr for HgCdTe, CaF_2 for InSb det.	U Nagoya, NIES
Boulder	BOU	Bruker 120/5 HR	KBr	NCAR
Tsukuba	TSU	Bruker 125 HR	KBr for HgCdTe, CaF_2 for InSb det.	NIES
Izaña	IZ	Bruker 120/5 HR	KBr	AEMet, KIT-ASF
Mauna Loa	MLO	Bruker 120/5 HR	KBr	NCAR
Altzomoni	ALT	Bruker 120/5 HR	KBr	UNAM
Wollongong	WOL	Bruker 125 HR	KBr	U Wollongong
Lauder	LAU	Bruker 120 HR & 125 HR	KBr	NIWA
Arrival Heights	AH	Bruker 125 HR	KBr	NIWA

155

https://doi.org/10.5194/amt-2020-316
Preprint. Discussion started: 4 September 2020

Atmospheric Measurement Techniques Discussions

These sites primarily serve the TCCON (Total Carbon Column Observing Network; Wunch et al., 2010) and just contribute with InSb spectra to NDACC and to this exercise. These spectrometers use a CaF_2 beam splitter instead of KBr; the latter is normally used in NDACC for enabling measurements in the HgCdTe spectral range. Ny-Ålesund, Paris, Rikubetsu and Tsukuba sites use a CaF_2 beam splitter for InSb and a KBr beam splitter for HgCdTe measurements. Tables 3 and 4 list the detected channeling frequencies and their amplitudes in spectra recorded with InSb and HgCdTe detectors, respectively.

4.1 InSb detector domain

Figure 3 shows the detected channeling frequencies and their amplitudes in InSb spectra analysed at about 2600 cm^{-1}. Most spectrometers show the expected channeling frequencies: about 0.9 cm^{-1} and 0.11 or 0.23 cm^{-1}. These frequencies are consistent with (i) the gap between beam splitter and compensator plate (0.9 cm^{-1}), and (ii) the beam splitter substrate (0.23 cm^{-1}; Table 1). A frequency of 0.11 cm^{-1} corresponds to a resonator due to both substrates, the beam splitter and the compensator plate.

A few spectrometers show an additional channeling fringe with a frequency of about 3 cm^{-1}. This is due to the detector window that is often made of sapphire or calcium fluoride (CaF_2). Also in Izaña, this channeling frequency was detected in 2018. In December 2018, the detector was exchanged because of decreasing sensitivity. The new detector (Izaña-2019) shows much less channeling. Detectors purchased in the 1990s sometimes had a detector window with insufficient wedge.

Figure 4 shows the amplitude of the strongest channeling frequency of each spectrometer. In most cases, channeling caused by the gap of the beam splitter is the most pronounced one. The amplitudes range from 0.1 to 2.0 ‰ with a mean of (0.68 +/- 0.48) ‰ and a median of 0.60 ‰. These mean and median are consistent with the PROFFIT error estimate of 0.5 ‰ as used in Vigouroux et al. (2018). However, the channeling amplitude differs strongly from spectrometer to spectrometer and a few spectrometers show an amplitude of up to 2 ‰.

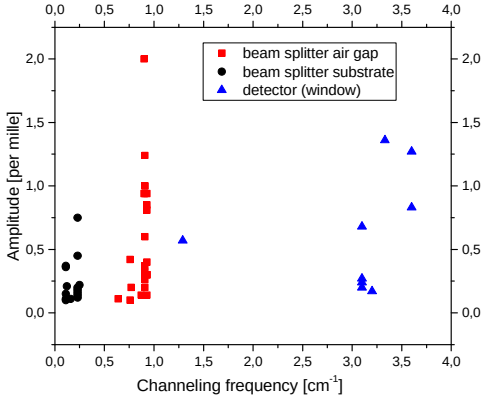

Figure 3: Amplitude of channeling frequencies as observed in InSb test spectra using NDACC filter no. 3.

https://doi.org/10.5194/amt-2020-316
Preprint. Discussion started: 4 September 2020

Atmospheric Measurement Techniques Discussions

Table 3: Leading channeling frequencies F and their amplitudes A in the InSb detector regime. Channeling amplitudes larger than 0.6 ‰ are highlighted in bold.

FTIR site	**F 1 [cm^{-1}]**	**A 1 [‰]**	**F 2 [cm^{-1}]**	**A 2 [‰]**	**F 3 [cm^{-1}]**	**A 3 [‰]**	**F 4 [cm^{-1}]**	**A 4 [‰]**
Eureka	0.93	0.14	0.23	0.05	0.11	0.004		
Ny-Ålesund	**0.90**	**2.0**	0.11	0.08				
Thule	**0.91**	**1.0**	0.23	0.18	0.11	0.15	3.1	0.27
Kiruna	0.85	0.05	0.11	0.003	0.76	0.1		
Sodankylä	0.93	0.3	0.12	0.03	0.11	0.024	0.25	0.01
Harestua	0.91	0.37	0.10	0.02	**3.33**	**1.36**		
St. Petersburg	0.93	0.3	0.23	0.12	0.16	0.11	0.77	0.20
Bremen	0.93	0.3	0.23	0.16	0.11	0.05		
Karlsruhe	0.87	0.14			1.29	0.57		
Paris	0.91	0.2	0.25	0.05				
Garmisch	0.91	0.6	0.10	<0.1	3.1	0.24		
Zugspitze	0.91	0.26	0.11	0.025	0.10	0.035		
Jungfraujoch	**0.91**	**1.24**	0.23	0.08	0.12	0.02		
Toronto	**3.10**	**0.68**	0.21	0.05	0.11	0.02		
Rikubetsu	**0.90**	**0.94**	0.25	0.22	0.11	0.11	3.2	0.17
Boulder	**0.93**	**0.81**	**0.23**	**0.75**	0.11	0.11	3.6	0.83
Tsukuba	**0.93**	**0.94**	0.12	0.21	0.11	0.10		
Izaña – 2018	0.76	0.42	0.10	0.09	0.11	0.06	**3.6**	**1.27**
Izaña – 2019	0.83	0.07	0.10	0.02	0.11	0.03	3.1	0.20
Mauna Loa	**0.93**	**0.85**	0.23	0.45	0.11	0.36		
Altzomoni	0.64	0.11	1.82	0.04	0.74	0.03		
Wollongong	0.93	0.40	0.23	0.20	0.11	0.03		
Lauder HR120	0.91	0.32	0.23	0.08	0.11	0.02		
Lauder HR125	**0.91**	**1.0**	0.23	0.14	0.11	0.37	0.10	0.06
Arrival Heights	**0.91**	**0.94**	0.23	0.03	0.12	0.11	0.10	0.09

https://doi.org/10.5194/amt-2020-316
Preprint. Discussion started: 4 September 2020

Atmospheric Measurement Techniques Discussions

Table 4: Leading channeling frequencies F and their amplitudes A in the HgCdTe detector regime. Channeling amplitudes larger than 1.0 ‰ are printed in bold.

FTIR site	F 1 [cm^{-1}]	A 1 [‰]	F 2 [cm^{-1}]	A 2 [‰]	F 3 [cm^{-1}]	A 3 [‰]	F 4 [cm^{-1}]	A 4 [‰]
Eureka	**0.93**	**1.5**	0.23	0.2	0.11 0.10	0.14 0.05		
Ny-Ålesund	**0.91**	**1.6**	0.23 **0.21**	0.89 **1.85**	0.11 0.10	0.60 0.62	**2.17**	**21**
Kiruna	0.77	0.32	0.59	0.12	0.11	0.07		
Harestua	**0.91**	**3.7**	0.23 0.11	0.73 0.16	1.56 0.58	0.66 0.36	**3.85**	**4.2**
St. Petersburg	**0.94**	**1.0**	0.23 0.33	0.30 0.40	2.0 1.77	0.52 0.20		
Bremen	**0.93** 0.83	**1.43** 0.52	0.23	0.34	0.11 0.10	0.22 0.08		
Paris	0.83	0.56	0.26 0.23	0.23 0.37	0.21 0.12	0.13 0.23		
Zugspitze	0.91	0.79	0.23	0.25	0.11 0.10	0.18 0.19	3.57	0.36
Jungfraujoch	0.91	0.53	0.23 0.21	0.60 0.12	0.11 0.10	0.17 0.06		
Toronto	0.96 0.48	0.64 0.12	0.21	0.20	0.10	0.10		
Rikubetsu	**0.93** **0.83**	**1.44** **1.51**	0.23 0.18	0.62 0.14	**0.11** **0.10**	**2.18** **1.01**	0.42	0.21
Tsukuba	**0.93**	**3.46**	0.23	0.67	0.11 0.10	0.38 0.33	1.19	0.27
Izaña – 2018	0.76	0.23	0.63 0.56	0.45 0.41	0.11 0.10	0.13 0.13		
Izaña – 2019	0.75	0.48	0.63	0.54	0.11	0.17		
Mauna Loa	**0.93**	**2.60**	0.23	**1.35**	0.11 0.10	0.56 0.10	0.61	0.14
Altzomoni	0.88 0.63	0.25 0.68	1.67 1.43	0.31 0.23	0.11	0.08	1.22	0.21
Wollongong	**0.93** 0.82	**3.00** 0.23	0.23 0.59	0.25 0.13	0.11	0.16		
Lauder HR120	0.91 1.51	0.72 0.08	0.23	0.06	0.11 0.10	0.12 0.07		
Lauder HR125	**0.91** **1.14**	**1.69** **2.74**	0.23	0.41	0.11 0.10	0.23 0.11		
Arrival Heights	**0.91** **1.16**	**1.72** **1.15**	0.23	0.18	0.11 0.10	0.12 0.17		

https://doi.org/10.5194/amt-2020-316
Preprint. Discussion started: 4 September 2020

Atmospheric Measurement Techniques Discussions

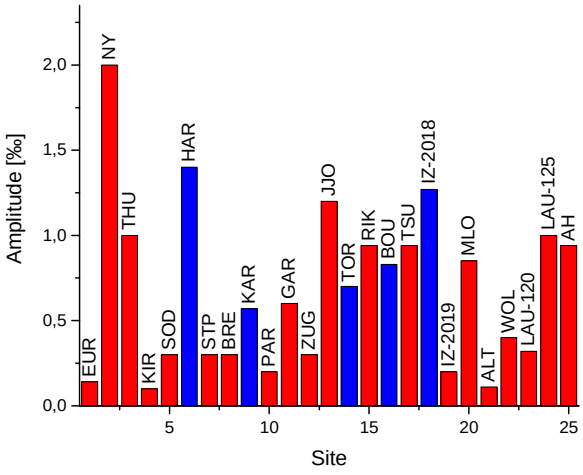

185 **Figure 4:** Amplitude of largest channeling fringe in test spectrum using InSb detector and NDACC filter number 3. Red bars indicate channeling due to beam splitter air gap and blue bars indicate detector window as source of channeling.

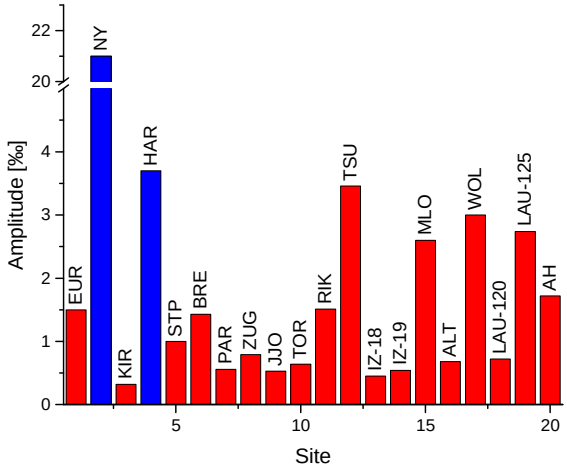

Figure 5: Amplitude of largest channeling fringe in HgCdTe test spectrum. Red bars indicate channeling due to beam splitter air gap and blue bars indicate detector window as source of channeling.

https://doi.org/10.5194/amt-2020-316
Preprint. Discussion started: 4 September 2020

Atmospheric Measurement Techniques Discussions

190 **4.2 HgCdTe detector domain**

Table 4 lists major channeling frequencies and their amplitudes in spectra recorded with an HgCdTe detector at about 1000 cm^{-1}. As for the InSb detector, most spectrometers show two dominant channeling frequencies: about 0.9 cm^{-1} and 0.1 or 0.2 cm^{-1} caused by the beam splitter (Table 1). Two spectrometers show an additional channeling frequency of 2.17 and 3.85 cm^{-1}, indicating that the wedge of the detector window is not sufficient in these cases.

195 Figure 5 shows the amplitude of the strongest channeling frequency of each spectrometer. In most cases, channeling caused by the gap of the beam splitter is the most pronounced one. The amplitudes range from 0.3 to 21 ‰ with a mean of (2.45 +/- 4.50) ‰ and a median of 1.2 ‰. The amplitude is even larger as compared to the InSb domain. At several sites, a reduction of channeling amplitudes would be desirable in order to improve trace gas retrievals of species with weak signatures, in particular from HgCdTe spectra, e.g. of $ClONO_2$, HNO_3 or SF_6.

200 As for the InSb domain, channeling amplitudes differ strongly from spectrometer to spectrometer. Figure 6 shows spectra with different levels of channeling of the same frequency (about 0.9 cm^{-1}) demonstrating the need of increasing the wedge of the gap and for narrowing the tolerances of wedges in the manufacturing of the beam splitters.

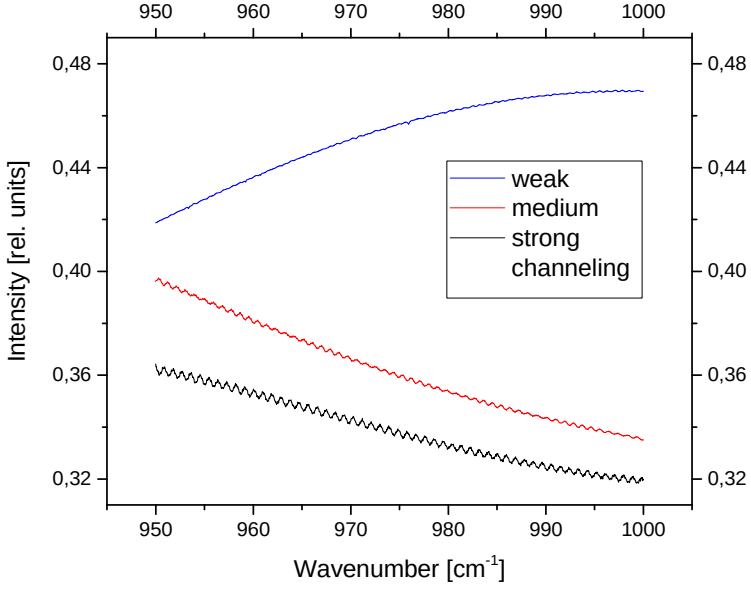

Figure 6: HgCdTe spectra with low (0.32 ‰), medium (1.43 ‰) and high (3.46 ‰) channeling amplitude at 0.9 cm^{-1} frequency.

https://doi.org/10.5194/amt-2020-316
Preprint. Discussion started: 4 September 2020

Atmospheric Measurement Techniques Discussions

205 **5 Investigation of a modified beam splitter design for reducing channeling**

This test exercise has found that the channeling amplitude differs strongly from spectrometer to spectrometer. A few spectrometers (at Altzomoni, Izaña, Karlsruhe and Kiruna) use customer-specific beam splitters with an increased wedge of 1.75° for the air gap and 10 arc min for the CaF_2 substrate and 8 arc min for the KBr substrate. Their channeling amplitudes are the lowest among all the spectrometers studied in this paper. Unfortunately, this type of beam splitter is not a standard
210 device and is not compatible with standard beam splitters, as it requires a realignment of the interferometer. Namely due to its incompatibility with far-infrared pellicle beam splitters, the manufacturer Bruker adheres to the standard design with lower substrate wedge.

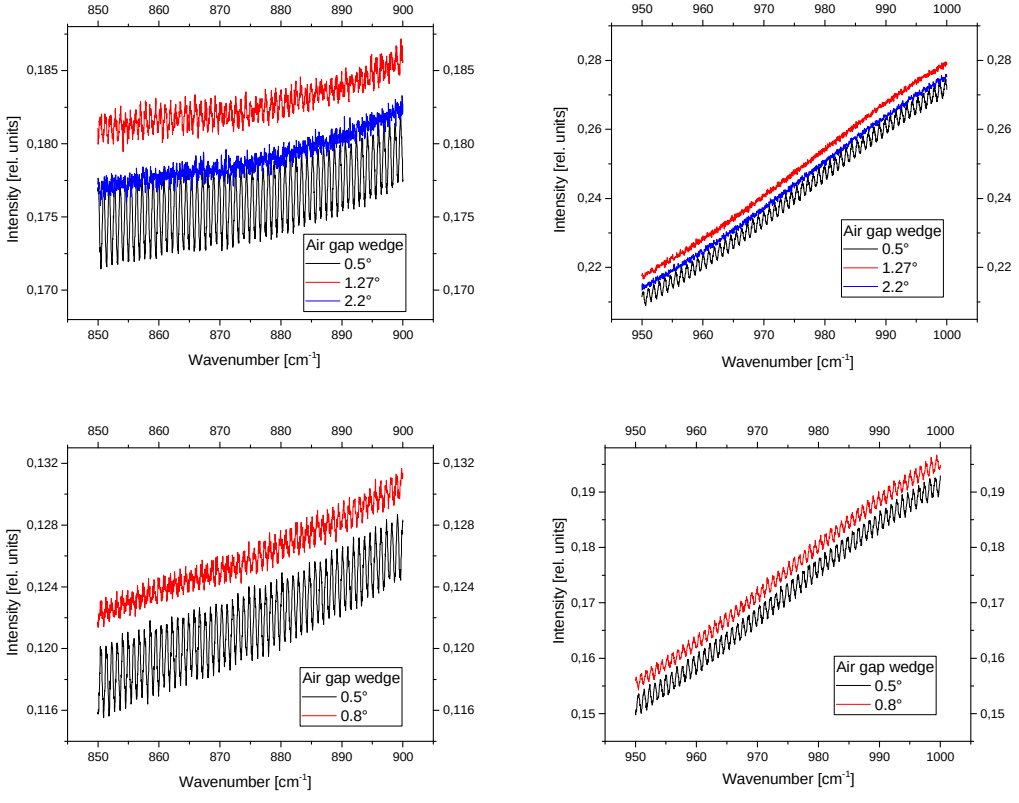

215

Figure 7: HgCdTe spectra recorded with different wedges of the air gap in between beam splitter and compensator plate for the 850 to 950 cm^{-1} and the 950 to 1000 cm^{-1} spectral ranges.

https://doi.org/10.5194/amt-2020-316
Preprint. Discussion started: 4 September 2020

Atmospheric Measurement Techniques Discussions

To avoid the need for strongly wedged substrates, a different approach is proposed here. We focus on the wedge of the gap between the beam splitter and the compensator plate. Since the largest channeling amplitude (at 0.9 cm^{-1} frequency) is caused by the air gap, an increased wedge of this gap has the potential to reduce channeling significantly. The typical air gap wedge for the Bruker beam splitter is 0.5°. Different spacers with wedges of 0.5°, 1.27° and 2.2° have been manufactured by Bruker and tested. Figure 7 (upper panels) shows the resulting channeling test spectra recorded with an HgCdTe detector. Similar to most of the NDACC spectrometers, the spectrum of the 0.5° wedged beam splitter shows a pronounced channeling with an amplitude of 5.7 ‰. In contrast, the 1.27° and 2.2° wedged beam splitters are (nearly) free of channeling with an amplitude of 0.46 and of 0.87 ‰, respectively, that is close to the noise level of these spectra . Analysed in the 850 to 900 cm^{-1} spectral range, the amplitude is 8.9, 3.3 and 0.6 ‰ for a wedge of 0.5°, 1.27° and 2.2°, respectively. For InSb spectra, the 0.9 cm^{-1} channeling generates amplitudes of 0.9, 0.45 and 0.19 ‰ for beam splitters with wedges of 0.5°, 1.27° and 2.2°, respectively. To ensure compatibility between different beam splitters, the wedge should be limited to 0.8°. This design will be implemented in future Bruker HR spectrometers. Figure 7 (lower panels) presents test spectra with an air gap wedge of 0.5° and 0.8°. In the 850 to 900 cm^{-1} spectral range, even the slightly increased wedge reduces the channeling by nearly 50 % (from 10 ‰ to 6 ‰). In the 950 to 1000 cm^{-1} range, however, the effect is smaller.

Moreover, this exercise demonstrates that a wedge of about 2° on the air gap eliminates channeling even without a larger wedge of the beam splitter substrate. However, such a spectrometer completely free of channeling would result in incompatibility with beam splitters having a smaller air gap wedge and therefore, the need to realign the spectrometer after a beam splitter exchange.

6 Conclusions

Firstly, this paper documents the channeling amplitudes for nearly all of the FTIR spectrometers used in NDACC. Such a systematic performance analysis is needed for improving the trace gas retrievals and for calculating complete error budgets. Within NDACC, laboratory test spectra of about twenty spectrometers were recorded and analysed. The derived channeling amplitudes range from 0.1 to 2.0 ‰ and from 0.3 to 21 ‰ in the InSb and HgCdTe domains, respectively. These values are not negligible when constructing the error budget of minor trace gases. A reduction of the channeling amplitudes is highly desirable for the analysis of gases like $ClONO_2$, HNO_3, HCHO, and SF_6.

Secondly, this study shows the potential to reduce channeling in several spectrometers and to improve the homogeneity within the network. The channeling frequencies allow us to determine the responsible optical component. A few instruments show channeling with a frequency of a few wavenumbers due to insufficiently wedged detector windows. Switching the detector window or, more easily, the entire detector including dewar and detector window, will help reduce channeling in these cases.

Finally, we found that most spectrometers show two dominant channeling frequencies with about 0.1 or 0.2 cm^{-1} and 0.9 cm^{-1} corresponding to beam splitter substrate and beam splitter air gap. In most cases, the channeling caused by the gap of the beam splitter is the leading one. The option of reducing this channeling contribution was investigated by adjusting the wedge angles on a test beam splitter. Increasing the wedge of this gap significantly reduces the channeling at 0.9 cm^{-1} and therefore, such a

https://doi.org/10.5194/amt-2020-316
Preprint. Discussion started: 4 September 2020

beam splitter design offers the promise of further reducing channeling. Switching to this modified beam splitter design would contribute to further homogenization of the spectrometers operated within NDACC.

Data availability. Channeling test spectra used in this study are available on request from the corresponding author (thomas.blumenstock@kit.edu).

Author contributions. TB designed the study, performed the analysis, and wrote the paper. FH designed the analysis of the test spectra. AK improved the beam splitter and provided test spectra. All other authors did lab measurements and provided test spectra. All authors read and provided feedback on the paper.

Competing interests. The authors declare no competing interests.

Acknowledgements. The authors like to acknowledge the project INMENSE (CGL2016-80688-P) funded by Ministerio de Economía y Competitividad from Spain. For the Altzomoni site UNAM (DGAPA grants IN111418 & IN107417), CONACYT (290589) and PASPA are acknowledged. The Paris site has received funding from Sorbonne Université, the French research center CNRS and the French space agency CNES. Operations at Rikubetsu and Tsukuba sites are supported in part by the GOSAT series project. SPbU team was supported by Russian Foundation for Basic Research through the project no.18-05-00011. The Lauder and Arrival Heights FTIR measurements are core-funded by NIWA through New Zealand's Ministry of Business, Innovation and Employment Strategic Science Investment Fund. We also thank Antarctica New Zealand for providing support for the FTIR measurements at Arrival Heights, which includes test spectra collection. The Jungfraujoch FTIR experiment has received funding from the F.R.S. – FNRS, the Fédération Wallonie-Bruxelles, both in Brussels, Belgium, and from the GAW-CH programme of MeteoSwiss. ULiège acknowledges that the International Foundation High Altitude Research Stations Jungfraujoch and Gornergrat (HFSJG), 3012 Bern, Switzerland, made it possible to carry out our experiment at the Jungfraujoch Station. We like to thank the AWI Bremerhaven and the personnel at the AWIPEV station, Ny-Ålesund (Spitsbergen) for logistic and on-site support. Eureka measurements were made at the Polar Environment Atmospheric Research Laboratory (PEARL), primarily supported by the Natural Sciences and Engineering Research Council of Canada (NSERC), Environment and Climate Change Canada, and the Canadian Space Agency. Toronto measurements were made at the University of Toronto Atmospheric Observatory (TAO), primarily supported by NSERC and the University of Toronto. The National Center for Atmospheric Research is sponsored by the National Science Foundation. The NCAR FTS observation programs at Thule, GR, Mauna Loa, HI and Boulder, CO are supported under contract by the National Aeronautics and Space Administration (NASA). The FTIR stations Bremen, Garmisch, Izaña, Karlsruhe, and Ny-Ålesund have been supported by the German Bundesministerium für Wirtschaft und Energie (BMWi) via DLR under grants 50EE1711A-B&D.

https://doi.org/10.5194/amt-2020-316
Preprint. Discussion started: 4 September 2020

The article processing charges for this open-access publication were covered by a Research Centre of the Helmholtz Association.

References

Abrams, M. C., Toon, G. C., and Schindler, R. A.: Practical example of the correction of Fourier-transform spectra for detector nonlinearity, Applied Optics, 33, 6307-6314, doi:10.1364/AO.33.006307, https://www.osapublishing.org/ao/abstract.cfm?URI=ao-33-27-6307, 1994.

De Mazière, M., Thompson, A. M., Kurylo, M. J., Wild, J. D., Bernhard, G., Blumenstock, T., Braathen, G. O., Hannigan, J. W., Lambert, J.-C., Leblanc, T., McGee, T. J., Nedoluha, G., Petropavlovskikh, I., Seckmeyer, G., Simon, P. C., Steinbrecht, W., and Strahan, S. E.: The Network for the Detection of Atmospheric Composition Change (NDACC): history, status and perspectives, Atmos. Chem. Phys., 18, 4935-4964, https://doi.org/10.5194/acp-18-4935-2018, 2018.

Dohe, S., V. Sherlock, F. Hase, M. Gisi, J. Robinson, E. Sepúlveda, M. Schneider, and T. Blumenstock: A method to correct sampling ghosts in historic near-infrared Fourier Transform Spectrometer (FTS) measurements, Atmos. Meas. Tech., 6, 1981-1992, doi:10.5194/amt-6-1981-2013, 2013.

Gisi, M., F. Hase, S. Dohe, and T. Blumenstock: Camtracker: a new camera controlled high precision solar tracker system for FTIR-spectrometers, Atmos. Meas. Tech., 4, 47-54, 2011.

Hase, F., T. Blumenstock, C. Paton-Walsh: Analysis of the instrumental line shape of high-resolution Fourier transform IR spectrometers with gas cell measurements and new retrieval software, Appl. Opt. 38, 3417-3422, 1999

Hase, F., J.W. Hannigan, M.T. Coffey, A. Goldman, M. Höpfner, N.B. Jones, C.P. Rinsland, S.W. Wood: Intercomparison of retrieval codes used for the analysis of high-resolution, ground-based FTIR measurements, Journal of Quantitative Spectroscopy & Radiative Transfer 87, 25–52, 2004.

Hecht, E.: Optics, Fifth Edition, Pearson Education, ISBN 978013397726, p. 440, 2017.

Keppel-Aleks, G., Toon, G.C., Wennberg, P.O., Deutscher, N.M.: Reducing the impact of source brightness fluctuations on spectra obtained by Fourier-transform spectrometry. Applied Optics. 46: 4774-9. PMID 17609726 DOI: 10.1364/AO.46.004774, 2007.

Messerschmidt, J., Macatangay, R., Notholt, J., Petri, C., Warneke,T., and Weinzierl, C.: Side by side measurements of CO_2 by ground-based Fourier transform spectrometry (FTS), Tellus B,62, 749–758,doi:10.1111/j.1600-0889.2010.00491.x, 2010.

Schneider, M. and F. Hase: Technical Note: Recipe for monitoring of total ozone with a precision of around 1 DU applying mid-infrared solar absorption spectra, ACP, Vol. 8, 63-71, SRef-ID: 1680-7324/acp/2008-8-63, 2008.

Vigouroux, C., Bauer Aquino, C. A., Bauwens, M., Becker, C., Blumenstock, T., De Mazière, M., García, O., Grutter, M., Guarin, C., Hannigan, J., Hase, F., Jones, N., Kivi, R., Koshelev, D., Langerock, B., Lutsch, E., Makarova, M., Metzger, J.-M., Müller, J.-F., Notholt, J., Ortega, I., Palm, M., Paton-Walsh, C., Poberovskii, A., Rettinger, M., Robinson, J.,

https://doi.org/10.5194/amt-2020-316
Preprint. Discussion started: 4 September 2020

Atmospheric Measurement Techniques Discussions

Smale, D., Stavrakou, T., Stremme, W., Strong, K., Sussmann, R., Té, Y., and Toon, G.: NDACC harmonized formaldehyde time series from 21 FTIR stations covering a wide range of column abundances, Atmos. Meas. Tech., 11, 5049-5073, https://doi.org/10.5194/amt-11-5049-2018, 2018.

Vigouroux, C., Langerock, B., Bauer Aquino, C. A., Blumenstock, T., Cheng, Z., De Mazière, M., De Smedt, I., Grutter, M., Hannigan, J., Jones, N., Kivi, Loyola, D., R., Lutsch, E., Mahieu, E., Makarova, M., Metzger, J.-M., Morino, I., Murata, I., Nagahama, T., Notholt, J., Ortega, I., Palm, M., Pinardi, G., Röhling, A., Smale, D., Stremme, W., Strong, K., Sussmann, R., Té, Y., van Roozendael, M., Wang, P., and Winkler, H.: TROPOMI/–Sentinel-5 Precursor formaldehyde validation using an extensive network of ground-based Fourier-transform infrared stations, Atmos. Meas. Tech., 13, 3751–3767, https://doi.org/10.5194/amt-13-3751-2020, 2020.

Wikipedia.org: https://en.wikipedia.org/wiki/Fabry-Perot_interferometer, last access on June 25, 2020; downloaded from Wikimedia Commons: https://commons.wikimedia.org.

Wunch, D., Toon, G. C., Wennberg, P. O., Wofsy, S. C., Stephens, B. B., Fischer, M. L., Uchino, O., Abshire, J. B., Bernath, P., Biraud, S. C., Blavier, J.-F. L., Boone, C., Bowman, K. P., Browell, E. V., Campos, T., Connor, B. J., Daube, B. C., Deutscher, N. M., Diao, M., Elkins, J. W., Gerbig, C., Gottlieb, E., Griffith, D. W. T., Hurst, D. F., Jiménez, R., Keppel-Aleks, G., Kort, E. A., Macatangay, R., Machida, T., Matsueda, H., Moore, F., Morino, I., Park, S., Robinson, J., Roehl, C. M., Sawa, Y., Sherlock, V., Sweeney, C., Tanaka, T., and Zondlo, M. A.: Calibration of the Total Carbon Column Observing Network using aircraft profile data, Atmos. Meas. Tech., 3, 1351–1362, https://doi.org/10.5194/amt-3-1351-2010, 2010.